Slip Detection and Control Using Tactile and Force Sensors

Claudio Melchiorri, *Member, IEEE*

***Abstract*—In this paper, some results concerning the detection and control of the relative motion (slippage) of two bodies in contact are presented. The main motivation of this research can be found in advanced manipulation with robotic systems, in which, depending on the particular task to be executed, it might be desirable either to avoid or to exploit the slippage of the manipulated object. The main contribution of this paper is that, besides the linear Coulomb friction effect, the rotational case is also addressed and, therefore, both translational and rotational motions are taken into account. This result is achieved by using an integrated sensor constituted by a force/torque and a tactile sensor. Experimental results are presented considering both the detection of the slippage and its subsequent control.**

***Index Terms*—Dexterous manipulation, force/torque sensors, slip detection and control, tactile sensors.**

I. Introduction

THE problem of measuring and exploiting the friction and the slippage during the interaction of a robotic device with its environment has always attracted considerable interest from the robotic community. Indeed, problems related to contacts and friction phenomena are very common in several areas of robotics, e.g., in manipulation with dexterous hands, in walking robots, in force control, in fixture devices *etc*., and obviously they must be considered in the task planning and control of the robotic system. Therefore, it is not surprising that a number of sensors and several techniques for measuring friction effects have been proposed both by the academic and industrial communities; see, e.g., the surveys given in [1]–[6].

An early contribution of how the proper use of sensors for measuring the contact state can improve the manipulation capabilities of robotic systems was given in [7]. After that, several researchers have demonstrated that the use of force/torque or tactile sensors can noticeably improve the manipulation capabilities of robotic systems. For example, in [8]–[10], it has been shown that a force/torque [also called intrinsic tactile (IT)] sensor can be adopted to increase the dexterity and robustness of robotic manipulation, while in [11]–[14] among many others, a tactile sensor has been exploited for the same purposes. Other interesting contributions relative to different aspects of the design and use of force and tactile sensors are given in [15]–[22].

Manuscript received October 25, 1999; revised June 6, 2000. Recommended by Guest Editors M. Kaneko and R. C. Luo. This work was supported in part by MURST (*RAMSETE* Project) and ASI.

The author is with the Department of Electrical Engineering, Computer Science and Systems, University of Bologna, I-40136 Bologna, Italy (e-mail: cmelchiorri@deis.unibo.it).

Publisher Item Identifier S 1083-4435(00)07823-6.

Very often, a *point contact* model is assumed, i.e., a punctual contact in which only linear forces can be applied. In this case, the friction constraint may oppose only a relative linear motion of the contacting objects, and nothing can be done to counteract a rotational motion. This is the well-known Coulomb friction model, that considers the normal and tangential forces applied at the "contact point." The ratio between these two forces, and in particular its maximum value, is classically defined as the linear friction coefficient μ_s. Only a few papers have considered the more general case of *soft finger* contacts, in which torques also can be applied about the normal direction to the contact area. In this case, a rotational motion about the normal direction of the contacting bodies also may be prevented by suitably applying a control force; see [14] and [23].

This paper addresses the above—mentioned problem; the main contribution presented here is a technique that allows, on the basis of proper sensorial equipment, the detection and the subsequent application of proper control actions in the case of combined linear and rotational slippage. To this purpose two types of sensors, a force/torque (IT) and a matrix tactile sensor, are considered. Experimental results show how their integrated use may allow a more general exploitation and control of the friction phenomenon.

This paper is organized as follows. In Section II, a brief description of the two sensors adopted in the experimental activity is given. In Section III, the most common models known in literature to describe the friction phenomenon are recalled, while in Section IV, the model used here for considering both the linear and rotational case is illustrated. Section V reports some experimental results for the detection and control of the slippage, while Section VI concludes with final remarks.

II. The Force/Torque and the Tacticle Sensor

In this section, the two sensors used for the experimental activity are briefly described. The IT force/torque sensor has been developed in the context of the University of Bologna, Bologna, Italy, robotic hand (UB-Hand) project [24], where the need for a distributed force sensoriality led to the design and development of miniaturized six-axes force sensors. The tactile matrix sensor has been designed and developed at the Delft University of Technology, Delft, The Netherlands [25]. Subsequently, it has been used in a number of different robotic applications for object recognition, slip detection, and grasp control [13].

A. Miniaturized Force/Torque Sensor

The sensing element of the device is realized by a light compliant mechanical structure with a parallelepiped shape [see Fig. 1(a)]. The sensor has been designed in such a way that

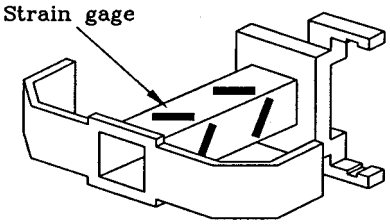

(a)

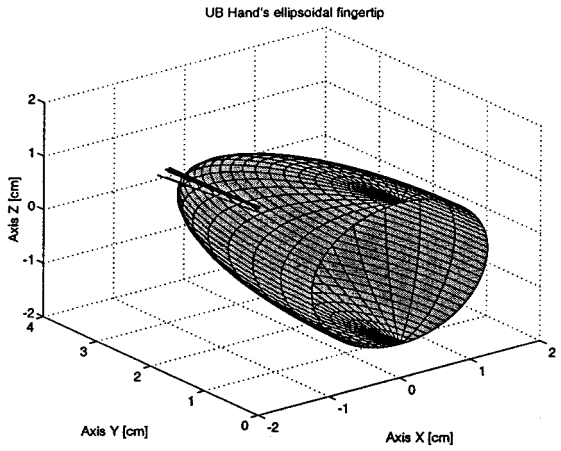

(b)

Fig. 1. (a) Sensing element of an IT sensor. (b) Forces applied at one of the fingertips of the UB-Hand and position of the contact point as measured by the sensor.

its base can be connected to the carrying robot link (phalange), while its upper part is rigidly connected to the external shell, e.g., the finger's surface; see [10]. Contact wrenches are mechanically transmitted to the elastic beam producing a deformation proportional to the amount of force, and eight strain gauges are used for measuring the entity of the deformation of the mechanical structure and for temperature compensation. The height, width, and depth of the sensor are 21, 24, and 15 mm, respectively.

This sensor enables measuring the components of wrenches applied to the robotic device, as well as the position of the contact point on it [see Fig. 1(b)] [10]. Other uses of this sensor concern the measurement of the linear static friction coefficient μ_s and the possibility of implementing proper strategies for controlling linear slippage, [6], [9].

B. Tactile Matrix Sensor

The tactile matrix sensor has been designed and manufactured at the Electronic Instrumentation Laboratory, Delft University of Technology [25]. The basic element of this sensor is a conductive rubber, whose resistance depends on the force applied on it.

Two electrodes, i.e., a "taxel,"[1] are necessary to measure the (local) resistance of the rubber. In fact, a current is driven by a constant voltage generator through the rubber from one electrode to the other. By measuring the current, it is possible to compute the resistance and, therefore, the force locally applied on the rubber. A printed circuit board of a $16 \times 16 = 256$ taxel matrix is used, with dimensions of approximately 2 cm $\times$ 2 cm, and with row and column strokes placed at equidistant positions (see Fig. 2). Note that the rubber, besides being used as a sensing element in the tactile sensor, may help in manipulation tasks for its frictional and elastic properties.

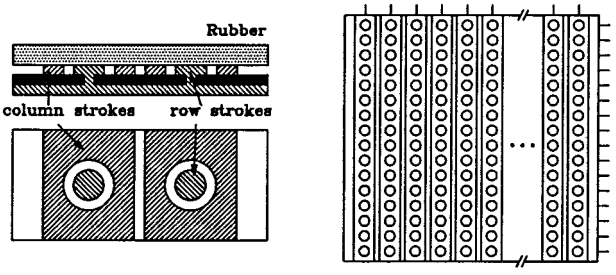

Fig. 2. Lateral and top views of two taxels and of the tactile sensor.

This sensor has been used for measuring the position and size of the contact area between a robotic finger and an object, as well as, from an analysis of the pressure distribution on the tactile pad, recognizing the shape of the object itself. More advanced applications of this sensor have been discussed in [11] and [13], where a technique for linear slippage detection has been presented. This technique is based on a frequency analysis of the information provided by the sensor.

III. Models of the Friction Effect

A. Model for Linear Load/Motion

The first studies on friction can be attributed to Leonardo da Vinci, although it was only with Coulomb in 1785 that a useful formulation of the friction laws was introduced, defining a relationship between the overall *friction force* $\boldsymbol{f}_f$ opposing the motion of two rigid bodies in contact and the *normal force* $\boldsymbol{f}_n$ acting between them.[2] The most common and simple description of the friction phenomenon considers two cases, i.e., *static* and *dynamic* (or *kinetic*) friction. With reference to Fig. 3, let us suppose that an external force $\boldsymbol{f}_t$ parallel to the contact plane is applied to one of the contacting bodies, and that a force $\boldsymbol{f}_n$ perpendicular to the contact plane is present, keeping the bodies in contact. A reaction force $\boldsymbol{f}_f$ due to the friction effect is generated and, in the static case, the following relationship holds between $\boldsymbol{f}_f$ and the normal force $\boldsymbol{f}_n$:

$$f_f \leq \mu_s f_n \tag{1}$$

where the static friction coefficient μ_s depends on the nature and the smoothness of the surfaces, and with good approximation can be considered independent of the size of the contact area. As is well known, (1) holds until the ratio f_f/f_n is less than or equal to the value of μ_s. In this case, the force f_f generated by friction is sufficient to balance any external force f_t and the

[1] *Taxel*, or "tactile pixel," is a term deriving from computer vision, and indicates a sensing element on the tactile pad of the sensor.

[2] In this paper, a bold symbol indicates a vector, while, when there is no ambiguity, the same symbol not in boldface is its magnitude: $f_t = |\boldsymbol{f}_t|$.

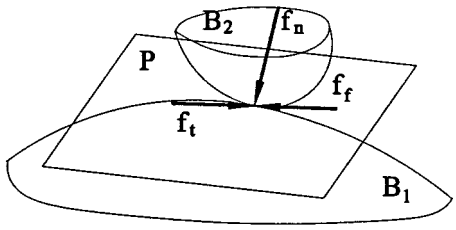

Fig. 3. Contact between two rigid bodies B_1 and B_2; P is the contact plane tangent both to B_1 and B_2, $\boldsymbol{f}_n$ is the normal force, $\boldsymbol{f}_t$ is an external load applied to one of the two bodies, and $\boldsymbol{f}_f$ is the friction force acting on P.

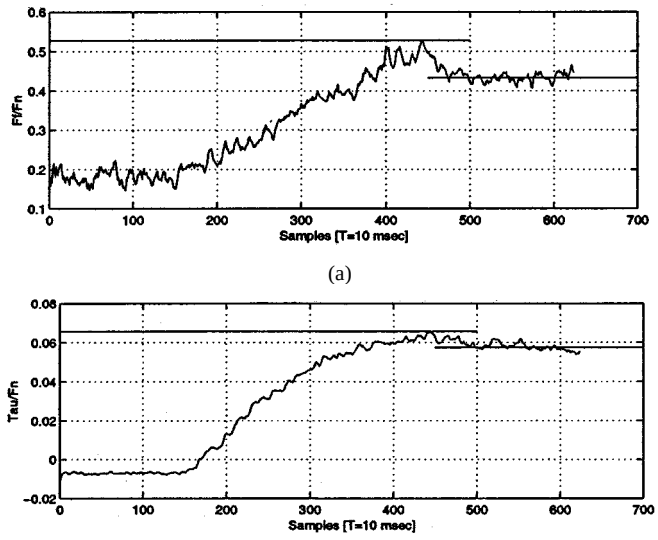

Fig. 4. Determination of the linear and rotational friction coefficient with a force sensor. (a) Plot of $\mu = f_f/f_n$. (b) Plot of $\beta = \tau_f/f_n$.

body does not move. If the external load f_t is increased, the body will eventually start sliding and the friction force f_f, opposing the motion, assumes a new value given by

$$f_f = \mu_d f_n \tag{2}$$

where μ_d is the dynamic friction coefficient. In general, $\mu_s > \mu_d$. A typical plot of the ratio f_f/f_n, i.e., of the friction coefficient μ, in a transition from a static to a dynamic situation is shown in Fig. 4(a), obtained by measuring the normal and tangential friction force components f_n and f_f in a contact situation. In this plot, the normal force component f_n is kept constant while an increasing external tangential force is applied until slippage takes place. The difference between the two values μ_s and μ_d can be clearly appreciated.

The case of rotational friction is more complex than the linear one. In fact, in general, a nonlinear relationship exists between the applied normal force f_n and the torque τ_f. This relationship may be expressed as [27]

$$\tau_f = 0.59\ \mu_s \alpha^{1/3}\ f_n^{4/3} = \beta_s' f_n^{4/3} \tag{3}$$

where α is a parameter depending on both the geometry and the elastic properties of the contacting bodies, such as the curvatures and the Young and Poisson moduli. If torques τ_f are in suitable ranges, (3) may be approximated with the linear relationship

$$\tau_f = \beta_s f_n. \tag{4}$$

Note that the friction coefficient β_s (or β_s') depends on the size of the contact area, and that this geometrical information cannot be provided by the force/torque sensor alone, although it can provide, for a given contact situation, information about the ratio τ_f/f_n. In Fig. 4(b), a typical result concerning this type of measurement is reported; an object is held with a constant normal force and an increasing external torque is applied. As in the linear case, a difference between the static and dynamic value may be appreciated. The plot shows a peak corresponding to the static coefficient β_s and then it decreases when the objects starts to move, corresponding to the dynamic friction coefficient $\beta_d = \tau_f/f_n$.

As already pointed out, in the case of rotations the knowledge of the normal and tangential forces f_n and f_t (or torque τ_f) alone is not sufficient and, therefore, a force sensor cannot provide a precise measurement of the phenomena between the two bodies. This type of sensor, in fact, provides only "global" information about the contact area, i.e., the resultant forces/torques. Therefore, in the case of rotation, a more detailed model of the contact forces must be defined, and additional types of sensors used.

B. Models for Linear and Torsional Loads/Motions

In the literature, some models have been proposed for describing the effects of a linear and torsional load in the contact area; see, e.g., [23], [26], and [28]. For practical applications, important issues are the simplicity and the adequacy of these models, which must be evaluated in real time. Among others, the model presented in [23] offers quite a simple test for a real-time implementation. In [23], in fact, several practical experiments have been presented, obtained using a finger equipped with a force sensor and applying to a grasped object proper combinations of forces and torques. The results are qualitatively summarized in plots a–d of Fig. 5(a).

These plots represent different conditions for testing a slipping condition between two objects; points outside one of these curves indicate that the friction forces are not sufficient to prevent relative motion.

In particular, plot d shows the case, nonreal, in which the effects of forces and torques applied on the object are decoupled; the object slips when $\tau > \tau_m = \beta_s f_n$ or when $f_t > f_m = \mu_s f_n$, i.e., the maximum allowed decoupled values due to friction constraints. Obviously, this is not the case in practice, and a coupling between the two actions is present and must be considered. Plot b reports the limit condition as deduced experimentally. The nonlinear relationship, as intuitive, points out that the maximum force (torque) decreases if an additional torque (force) is applied. Plots a and c are approximations of plot b, useful for real-time implementation of this technique. In particular, plot a) is the linear approximation given by

$$\frac{f_t}{\mu_s} + \frac{\tau}{\beta_s} = f_n \tag{5}$$

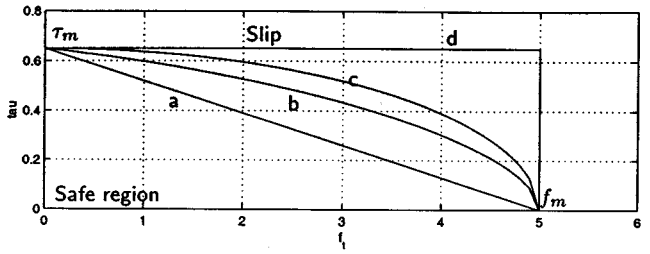

(a)

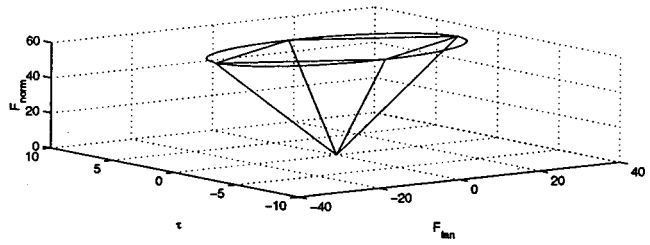

(b)

Fig. 5. (a) Qualitative limit curves for torsional/linear loading: *a*: linear approximation; *b*: calculated values; *c*: elliptical approximation; *d*: decoupled shear and moment (obtained with the values: $\mu_s = 0.5$, $\beta = 0.065$, $f_n = 10N$); (b) friction limit, see (5), in the 3-D space $\{f_t, \tau, f_n\}$ for different values of f_n.

while plot c is the elliptical approximation computed as

$$\frac{f_t^2}{\mu_s^2} + \frac{\tau^2}{\beta_s^2} = f_n^2. \tag{6}$$

In this manner, simple conditions are obtained for the detection of a slip condition. On the other hand, implicit drawbacks of this technique are the fact that it is based only on global information, i.e., the overall force and the torque, and that it is not simple to have a good estimation of the rotational friction coefficient β_s, since it depends on the size of the contact area, that is unmeasurable with force sensors alone.

IV. Model for Translational and Rotational Slip Detection

When only linear forces are applied at the contact, and considering a Coulomb friction model with static coefficient μ_s, from (1) a simple condition to check if a relative motion between two bodies takes place consists in verifying the inequality

$$\frac{f_f}{f_n} \le \mu_s \quad \Longrightarrow \quad \frac{\sqrt{f_{fx}^2 + f_{fy}^2}}{f_n} \le \mu_s. \tag{7}$$

This simple method has been successfully used in several experiments for slip detection and control using an IT sensor; see, e.g., [6], [9], and also the experimental part in Section V.

On the other hand, this condition is not sufficient when the forces acting on the object generate a torque component on it. As a matter of fact, as already pointed out, in this case a more general relationship must be defined and used, since it is not possible to define a simple and linear equation such as (1) and, moreover, the geometry of the contact area must also be considered. For these reasons, as also suggested in [14], we consider in the following the integrated use of an IT and a tactile matrix sensor like those described in Section II.

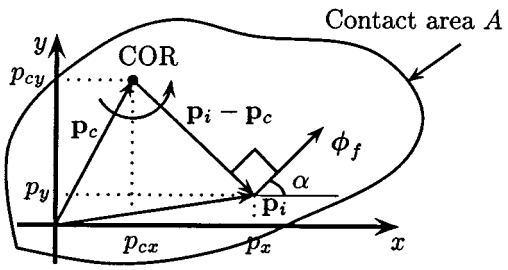

Fig. 6. At the limit condition, the direction of the local friction force ϕ_f is perpendicular to $\boldsymbol{p}_i - \boldsymbol{p}_c$.

In general, the motion of a rigid body in contact with a surface is a rotation about a point called *center of rotation* (COR). A particular case is when this point is at infinity, and the motion reduces to a pure translation. With reference to Fig. 6, define a reference frame $\mathcal{F}$ fixed with respect to the tactile pad, and indicate as ϕ_f the friction force locally active at a generic point $\boldsymbol{p}_i$ of the contact area. When the body starts to slide, since the motion is a rotation about the COR, the direction of ϕ_f is perpendicular to the vector joining the COR with $\boldsymbol{p}_i$, i.e., $\phi_f^T(\boldsymbol{p}_i - \boldsymbol{p}_c) = 0$ (see Fig. 6).

A practical approach to test the slip condition is reported in the following. Let us suppose that the COR position $\boldsymbol{p}_c = [x_c, y_c]^T$ is known with respect to $\mathcal{F}$. Moreover, we consider using both a force/torque sensor, giving the normal and tangential force $\boldsymbol{f}_n$ and $\boldsymbol{f}_t$ and the overall torque τ_t, and tactile matrix sensor, measuring the size and shape of the contact area A and the distribution of local pressure. Note that from the combination of the two sensors, it is possible to evaluate also the local normal forces ϕ_n in each taxel of the tactile sensor.

At the limit condition, it is therefore possible to compute the torque τ_c about z, the direction perpendicular to the contact surface. As a matter of fact, τ_c is computed by the friction forces acting on A with respect to the COR as

$$\begin{aligned}\tau_c &= \int_A |\phi_f \times (\boldsymbol{p}_i - \boldsymbol{p}_c)|\, dA \\ &= \int_A \mu_s \phi_n \sqrt{(p_x - p_{cx})^2 + (p_y - p_{cy})^2}\, dA\end{aligned} \tag{8}$$

or, since the tactile sensor provides only "discrete" data on the tactile pad in points corresponding to the taxels, as

$$\tau_c = \sum_{i=1}^{256} \mu_s \phi_{n,i} \sqrt{(x_i - x_c)^2 + (y_i - y_c)^2} \tag{9}$$

where 256 is the total number of taxels of the sensor. Then, it is possible to compare τ_c with the torque τ_t measured by the force sensor. No rotational motion takes place between the two bodies if the following inequality holds:

$$\tau_t \le \tau_c = \sum_{i=1}^{256} \mu_s \phi_{n,i} \sqrt{(x_i - x_c)^2 + (y_i - y_c)^2}. \tag{10}$$

Note that, in general, an external force $\boldsymbol{f}_t$ can be applied to the object and that, therefore, the condition to be tested in order to check if slippage takes place becomes

$$|\tau_t + \boldsymbol{f}_t \times \boldsymbol{p}_c| \le \mu_s \sum_{i=1}^{256} \phi_{n,i} \sqrt{(x_i - x_c)^2 + (y_i - y_c)^2}. \tag{11}$$

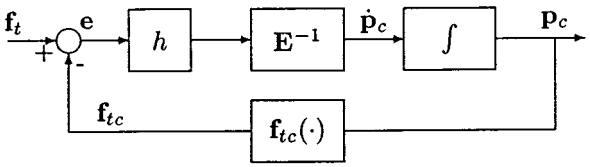

Fig. 7. Block diagram representation of the adopted numerical technique.

From a theoretical point of view, in this manner it is possible to verify if a slippage takes place, verifying at the same time, knowing the COR position, if it consists of a rotation, a pure translation, or of a combination of the two.

From the above, since the quantities τ_t, $\boldsymbol{f}_t$ and $\phi_{n,i}$ are known from the two sensors, it follows that the problem reduces to the determination of $\boldsymbol{p}_c$, the COR position, from which by means of (9) it is possible to compute τ_c.

In practice, once the external tangential force $\boldsymbol{f}_t = [f_{tx},\ f_{ty}]^T$ acting on the body is known, as well as the distribution of the local force components ϕ_f and ϕ_n and the geometry of the contact area A, the COR position $\boldsymbol{p}_c$ can be computed from the following equations (see also Fig. 6):

$$\begin{cases} f_{tx} = -\displaystyle\sum_{i=1}^{256} \frac{\mu_s \phi_{n,i}(y_i - y_c)}{\sqrt{(x_i - x_c)^2 + (y_i - y_c)^2}} \\ f_{ty} = \displaystyle\sum_{i=1}^{256} \frac{\mu_s \phi_{n,i}(x_i - x_c)}{\sqrt{(x_i - x_c)^2 + (y_i - y_c)^2}} \end{cases} \tag{12}$$

where x_i, y_i is the position of the ith taxel. Equations (12) allow computing the unknown COR position, i.e., x_c, y_c. Note that we have assumed in (12) a constant friction coefficient in each point of the contact surface: $\mu_i = \mu_s$. Moreover, note that these equations are valid only at the limit condition for slippage, i.e., when $|\phi_f| = \mu_s \phi_n$. On the other hand, the computation of the COR position makes sense only after the slip motion begins, since the relative motion of the objects is null beforehand.

The possibility that the COR coincides with one of the taxels of the tactile sensor must be explicitly considered, since in this case (12) cannot be used. Each taxel must be evaluated as a possible COR, verifying that the following equations:

$$\begin{cases} f_{tx} = \phi_{jx} - \displaystyle\sum_{i \neq j}^{256} \frac{\mu_s \phi_{n,i}(y_i - y_c)}{\sqrt{(x_i - x_c)^2 + (y_i - y_c)^2}} \\ f_{ty} = \phi_{jy} + \displaystyle\sum_{i \neq j}^{256} \frac{\mu_s \phi_{n,i}(x_i - x_c)}{\sqrt{(x_i - x_c)^2 + (y_i - y_c)^2}} \end{cases}$$

where ϕ_{jx}, ϕ_{jy} are the (unknown) tangential force components in the jth taxel, are satisfied with

$$\sqrt{\phi_{jx}^2 + \phi_{jy}^2} \leq \mu_s |\phi_{n,j}|.$$

In order to solve the nonlinear equations (12) in the unknowns x_c, y_c, a recursive technique has been adopted, similar to a method presented in the literature for the solution of the inverse kinematic problem or the control of robot manipulators [29]. This technique is based on the block diagram of Fig. 7, where $\boldsymbol{E} = \partial \boldsymbol{f} / \partial \boldsymbol{p}_c$ is the Jacobian matrix of function $\boldsymbol{f}_t(\boldsymbol{p}_c)$, i.e., of equations (12), and h is a proper gain. For a detailed description and for the stability and convergence proof of this technique, see [29].

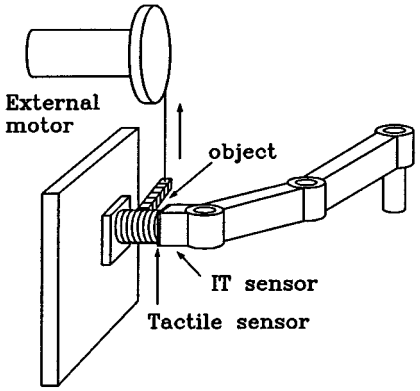

Fig. 8. Laboratory setup with the 2-DOF planar "finger" and a motor to apply forces to the grasped object. The joint connecting the sensor to the finger is idle; objects of different shapes have been used.

The relationship (11) represents an extension of (7) to the case of both forces and torques applied at the contact, and is more general than (5) and (6) since it takes into consideration the size of the contact area and avoids the computation of the rotational friction coefficient β_s.

V. Experimental Results

A laboratory setup has been prepared for testing the methodologies described in the previous section. The setup consists basically in a planar two-degrees-of-freedom (2-DOF) "finger," with a "fingertip" equipped with the IT and the tactile sensors, a fixed surface on which an object can be held, and an external motor, with a precision position sensor, suitable for applying forces/torques to the object and measuring its displacement (see Fig. 8). Different rigid objects can be used, and the external motor can be used to apply both forces and torques on them, i.e., to generate both linear and rotational motions.

Several experiments have been carried out in order to demonstrate the possibilities given by these sensors. Part of this activity has already been presented in [10] for the force/torque sensor, and in [11] and [13] for the tactile sensor.

The results reported in this section refer to two cases in detecting slippage between two bodies. The first case concerns the detection and control of linear slippage, and is based on the use of the IT sensor only. The second case refers to the detection of the combination of linear and rotational slip. Two types of experiment are reported in this case, involving the use of the IT sensor alone and the integration of the IT and the tactile sensors.

A. Translational Slip Detection and Control

If the friction coefficient is known, e.g., by means of a measurement as in Fig. 4, it is possible to use it in manipulation strategies in order, for example, to prevent slippage of the object.

The simplest control strategy for avoiding slippage is to use (7) to compute in real time the normal force f_n needed to balance the applied tangential force f_t. A more convenient solution consists in adopting a conservative scaling factor $\sigma \leq 1$ for the friction coefficient. Moreover, it may be necessary to bound the computed value of f_n in order to neglect measurement noise and

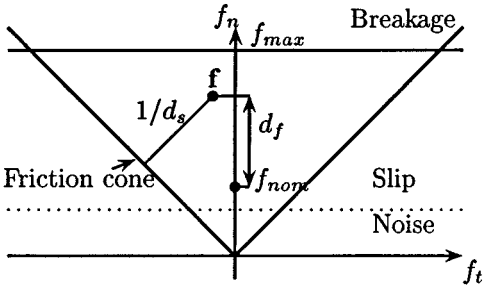

Fig. 9. Goals of the control strategy are minimization of d_s and d_f.

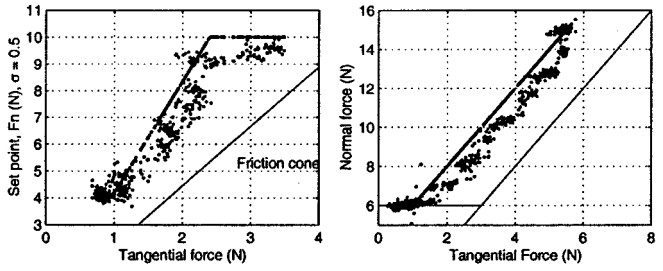

(a) (b)

Fig. 10. Linear slip control with (a) $\sigma = 0.5$, and (b) from [9].

to avoid the application of high forces. Therefore, the normal force f_n is computed as

$$f_{n1} = \frac{f_t}{\sigma \mu_s}$$
$$f_{n2} = \max\{f_{n1},\, f_{\rm nom}\}$$
$$f_n = \min\{f_{n2},\, f_{\max}\}$$

where $f_{\rm nom}$ is the nominal force to be applied when no tangential components are present, and $f_{\max}$ is the maximum applicable value. The results obtained with this technique are shown in Fig. 10. Each dot represents the applied normal force as a function of the tangential force, and the diagonal lines represent the border of the friction cone; slip is always avoided. The measured friction coefficient in the experiments was $\mu_s = 0.45$.

A similar strategy to prevent slippage was proposed in [9]; with reference to Fig. 9, where the friction cone is schematically shown, the goals are to maximize the distance of the representative point $\boldsymbol{f}$ of the applied force from the slip situation, i.e., $1/d_s$, and to minimize its distance d_f from the nominal set point $f_{\rm nom}$. A typical result of this technique is reported in Fig. 10. Slippage is avoided with a different slope for the desired normal force f_n; in general, a lower value for f_n is required.

B. Detection and Control of Linear and Rotational Slip

Experiments are now presented showing the possibilities given by the two integrated sensors for the detection and control of the rotational slippage.

1) Using Only the IT Sensor: Similarly to the linear case, experiments have been performed to verify the applicability of a slippage avoidance strategy also for the torsional case. Using the IT sensor alone, a "measure" of the rotational friction coefficient β_s has been obtained, as shown in Fig. 4(b), and used for slip control.

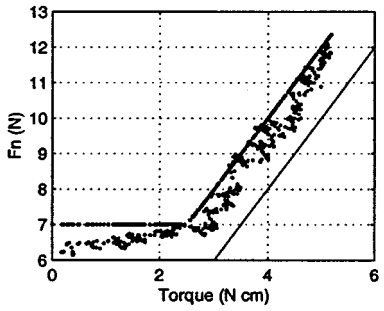

Fig. 11. Control of rotational slippage according to (13), $k = 2N$.

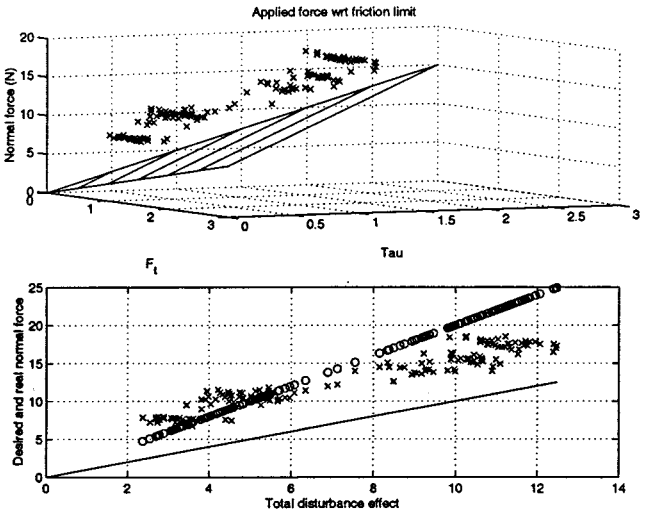

Fig. 12. Desired and applied normal forces in the 3-D space $\{f_t,\, \tau,\, f_n\}$, see Fig. 5(b), and a 2-D projection on plane $\{(f_t/\mu_s + \tau/\beta_s),\, f_n\}$. The circles are the set points.

When both forces and torques are applied at the contact, a conservative condition on the normal force [see (5)] is

$$\beta_s f_t + \mu_s \tau \le \beta_s \mu_s f_n.$$

Similarly to the linear case, the desired normal force may be computed as

$$f_{n1} = \max\left\{\frac{f_t}{\mu_s} + \frac{\tau}{\beta_s} + k,\, f_{nom}\right\}, \quad f_n = \min\{f_{n1},\, f_{\max}\} \tag{13}$$

where $k \ge 0$ is a proper safety factor. In Fig. 11, a typical result is shown, in a case in which only external torques are applied to the object. The diagram reports the normal force as a function of the applied torque. Again, it may be seen that slippage may be avoided.

A more general case is shown in Fig. 12, where both external torques and forces are applied to the object. Fig. 12 shows the applied normal force referred to the friction plane [in the space $\{f_t,\, \tau,\, f_n\}$, see Fig. 5(b)] and its two–dimensional (2-D) projection on plane $\{(f_t/\mu_s + \tau/\beta_s),\, f_n\}$. The control action f_n has been computed as

$$f_n = \frac{1}{\sigma}\left(\frac{f_t}{\mu_s} + \frac{\tau}{\beta_s}\right)$$

where σ is a conservative value (0.5 in the this experiment).

2) Using Both the Sensors: Two experiments are now presented with the approach illustrated in Section III-A. The first

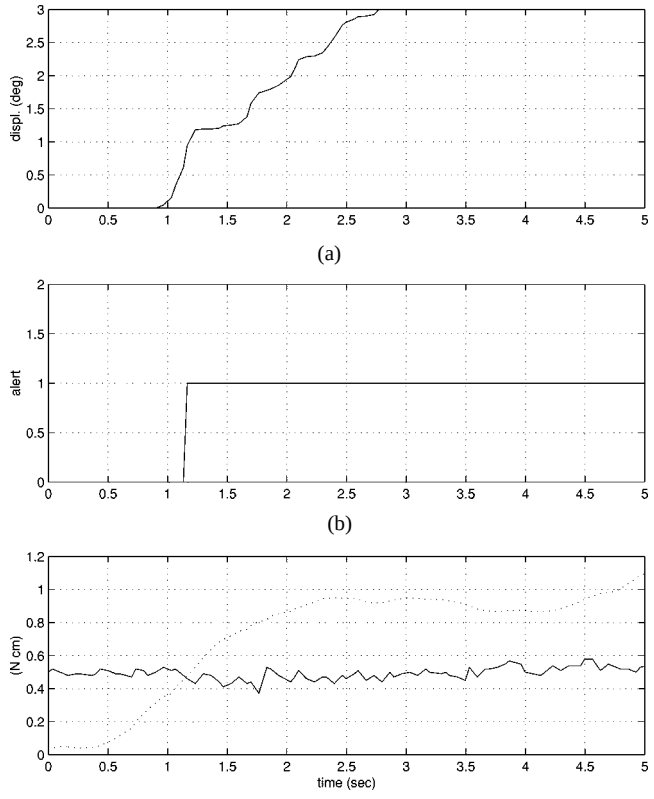

Fig. 13. Experiment with known COR position. (a) rotational displacement. (b) Result of condition (11) (1 = slippage). (c) Torques τ_c (solid) and τ_t (dotted).

consists in testing inequality (11) when the COR position is known in advance, while the second presents a more realistic situation that implies the computation of the COR position in real time.

a) Known COR Position: This experiment is reported to show, when the COR position is known, the possibility of identifying the slippage of a grasped object by means of (11). For this reason, it is straightforward to verify that, if the tangential force components f_{tx}, f_{ty} applied to the object are null, the COR position coincides with the *center of pression* (CP) on the tactile sensor (x_p, y_p). In fact, in this case, from (12) one obtains

$$f_{tx} = -\sum_{i=1}^{256} \frac{\mu_s \phi_{n,i}(y_i - y_c)}{\sqrt{(x_i - x_c)^2 + (y_i - y_c)^2}} = 0$$

from which

$$y_c = \frac{\sum_{i=1}^{256} \phi_{n,i} y_i}{\sum_{i=1}^{256} \phi_{n,i}} = y_p$$

and similarly for x_c. In order to be sure that only pure torques are applied to the object and, therefore, that the COR position is known, the object has been constrained with a device that allows only pure rotational motions.

In Fig. 13, a typical result is shown. In Fig. 13(a), the angular displacement of the object about the COR is reported as a function of time. The result of condition (11) is shown in Fig. 13(b). The value 1 means that (11) is not satisfied and, therefore, a motion is taking place, as shown in Fig. 13(a). Finally, in Fig. 13(c), the torque originated by the friction forces τ_c, computed by (9), and the external torque τ_t are reported. Since the applied normal force f_n is constant, τ_c also results as approximately constant. It is clear that it is possible to detect the slippage only after (11) is violated and, therefore, only after a (small) rotational displacement has occurred. Nevertheless, by modifying the value of f_n, proper control actions can be considered at this point in order to control or stop the slippage.

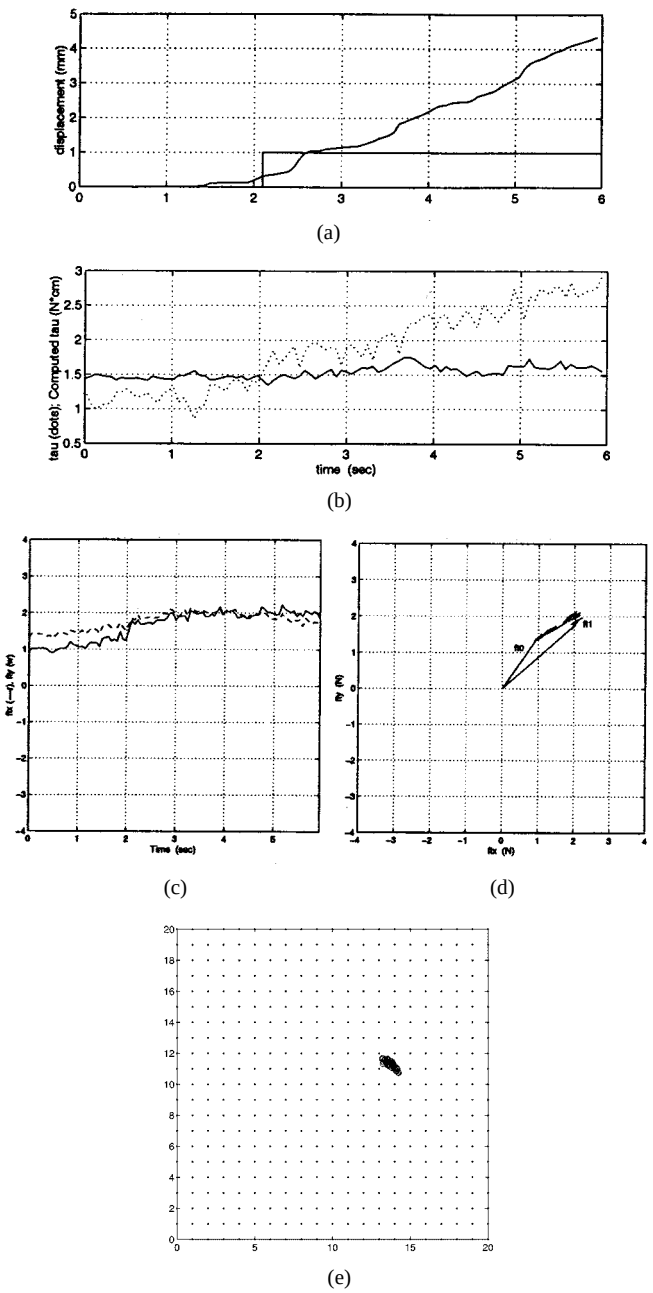

Fig. 14. Experiment with unknown COR position. (a) Rotational displacement and result of condition (11) (1 = slippage). (b) Torques τ_c (solid) and τ_t (dotted). (c) x–y components of the measured tangential force. (d) Behavior of $\boldsymbol{f}_t$. (e) Computed COR position on the tactile pad.

b) Unknown COR Position: In general, the COR position is not known and must be computed in real time.

Results obtained in this case are reported in Fig. 14, reporting the displacement, the "alert" signal, and the torques τ_c (com-

puted by the algorithm) and τ_t (measured by the IT sensor). Moreover, the tangential force components f_{tx}, f_{ty}, the whole vector $\boldsymbol{f}_t$ and the computed COR position on the tactile pad are shown. Note that, in this case, the displacement is a composition of both a rotational and a linear motion, since in this case the object is not constrained by any mechanical device.

3) Rotational and Translational Slip Control: Since it is possible to detect the slip between the two contacting bodies, it is possible to apply a control action similarly to the translational case. The condition to be checked is (11). For the sake of simplicity, we assume that the variation δf_n of the normal force f_n applied by the robotic finger is uniformly distributed on the contact area A, i.e., all the local normal force components $\phi_{n,i}$ change by the same amount $\delta\phi_n = \delta f_n/N$. Moreover, we define

$$n_t = |\tau_t + \boldsymbol{f}_t \times \boldsymbol{p}_c, | \quad \delta f_n = \sum_{i=1}^{256} \delta\phi_{ni}.$$

Therefore, we obtain from (11)

$$n_t \leq \sum_{i=1}^{256} \mu_s \delta\phi_n \sqrt{(x_i - x_c)^2 + (y_i - y_c)^2}$$

and, with the introduction of a conservative factor σ, when (11) does not hold the desired variation δf_n of the normal force may be computed as

$$\delta f_n = \frac{n_t - \tau_c}{\sigma\mu_s \sum_{i=1}^{256} \sqrt{(x_i - x_c)^2 + (y_i - y_c)^2}}. \qquad (14)$$

The results obtained with the above control strategy are shown in Fig. 15. In the figure, one may appreciate both the increase in the normal force f_n when the external disturbance is applied and the fact that slippage is resisted. In particular, in Fig. 15(b), the results are compared with the ideal plane in the space $\{f_t, \tau, f_n\}$ as in Fig. 12, although this definition is not used now. This comparison between the two control modalities shows in particular that in this case stability may be ensured with lower values of the grasping force f_n.

Note that the fact of using both the sensors allows avoiding the measurement of β, the rotational friction coefficient, which depends on the size of the contact area A and, therefore, may change during task execution. Moreover, as already pointed out, note that the object may be constrained using smaller values of the normal force, i.e. the technique based only on the IT sensor provides more conservative control actions.

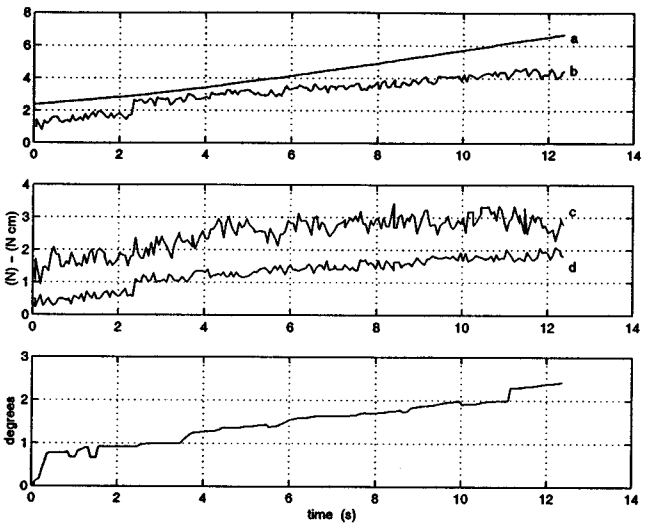

(a)

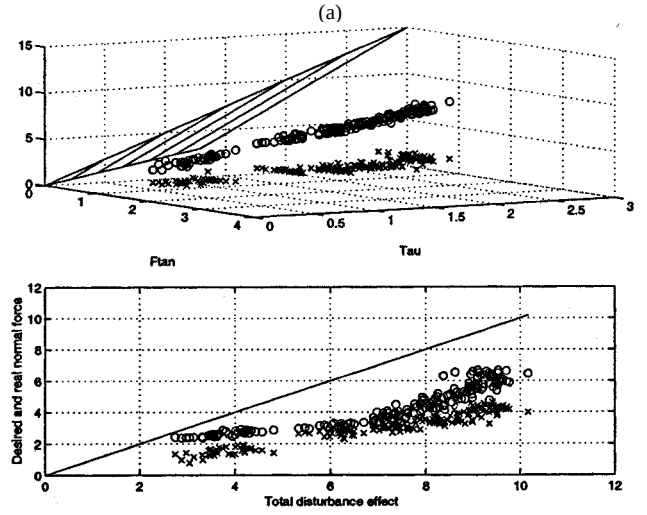

(b)

Fig. 15. Rotational and translational slip control using both sensors. (a) Plots *a*: set point and *b*: real normal force; *c*: disturbance force and *d*: torque; measured angle of displacement. (b) Plots show the desired set point (circles) and the real normal force referred to the friction plane (in the space $\{f_t, \tau, f_n\}$) and their projection on plane $\{(f_t/\mu_s + \tau/\beta_s), f_n\}$.

VI. Conclusions

In this paper, the problem of detecting and controlling rotational and linear slip in interaction tasks with robotic devices has been addressed. For this purpose, the integrated use of a force/torque and of a tactile matrix sensor has been discussed, as well as the exploitation of these devices for the detection of a slip condition and for the subsequent control. This problem is of interest in robotics for the implications in advanced manipulation tasks, where the slippage of the manipulated object could be avoided or even exploited by applying proper grasping forces at the contact points. For this purpose, a control strategy already successfully applied for controlling translational displacements has been modified for the case in which both rotations and linear displacements are present. Experimental results show the effectiveness of the control strategy for this more general case. The basic requisite is the knowledge of the friction coefficient μ_s, which can be easily measured by the force/torque sensor. Other information about the contact state, i.e., forces/torques and size of the contact area can be obtained with the use of the two sensors. Current activity deals with the exploitation of the friction effect for controlling in a desired manner the motion of a grasped object. Moreover, future work will address grasp stability analysis and micromanipulation capabilities by means of robotic hands.

Acknowledgment

The author wishes to thank C. Bonivento, G. Vassura, and L. Marconi for their contributions to this work.

REFERENCES

[1] A. Pugh, *Robot Sensors, Vol. 2: Tactile and Non-Vision*. Berlin, Germany: Springer-Verlag, 1986.

[2] H. R. Nicholls and M. H. Lee, "A survey of robot tactile sensing technology," *Int. J. Robot. Res.*, vol. 8, no. 3, pp. 3–30, June 1989.

[3] R. S. Fearing, "Tactile sensing mechanisms," *Int. J. Robot. Res.*, vol. 9, no. 3, pp. 3–23, 1990.

[4] M. H. Lee and H. R. Nicholls, "Tactile sensing for mechatronics—A state of the art survey," *Mechatron.*, vol. 9, pp. 1–31, 1999.

[5] J. Webster, Ed., *Tactile Sensors for Robotics and Medicine*. New York: Wiley, 1988.

[6] W. Jongkind and C. Melchiorri, "Tactile sensing for robotic manipulation," presented at the IEEE Int. Conf. Robotics and Automation, Minneapolis, MN, Apr. 22–28, 1996.

[7] J. K. Salisbury, "Interpretation of contact geometries from force measurements," in *Proceedings of the 1st International Symposium on Robotic Research*, M. Brady and R. Paul, Eds. Cambridge, MA: MIT Press, 1984.

[8] A. Bicchi and P. Dario, "Intrinsic tactile sensing for artificial hands," in *Robotics Research*, R. Bolles and R. Roth, Eds. Cambridge, MA: MIT Press, 1987.

[9] A. Bicchi, "Intrinsic contact sensing for soft fingers," in *Proc. IEEE Conf. Robotics and Automation*, Cincinnati, OH, May 1990, pp. 968–973.

[10] A. Cicchetti, A. Eusebi, C. Melchiorri, and G. Vassura, "An intrinsic tactile force sensor for robotic manipulation," in *Proc. 7th. Int. Conf. Advanced Robotics, ICAR'95*, Sant Feliu de Guixols, Spain, Sept. 20–22, 1995, pp. 889–894.

[11] E. G. M. Holweg, H. Hoeve, W. Jongkind, L. Marconi, C. Melchiorri, and C. Bonivento, "Slip detection by tactile sensors: Algorithms and experimental results," in *Proc. IEEE Int. Conf. Robotics and Automation*, Minneapolis, MN, Apr. 22–28, 1996, pp. 3234–3239.

[12] M. R. Tremblay and M. R. Cutkosky, "Estimating friction using incipient slip sensing during a manipulation task," in *Proc. 1993 IEEE Int. Conf. Robotics and Automation*, 1993, pp. 429–434.

[13] L. Marconi and C. Melchiorri, "Incipient slip detection and control using a rubber-based tactile sensor," in *IFAC'96 World Congr.*, San Francisco, CA, June 30–July 5, 1996, pp. 475–480.

[14] A. Bicchi, M. Bergamasco, P. Dario, and A. Fiorillo, "Integrated tactile sensing for gripper fingers," in *Proc. 7th Int. Conf. Robot Vision and Sensory Control, RoViSec'88*, Zurich, CH, 1988, pp. 339–349.

[15] R. D. Howe, "Tactile sensing and control of robotic manipulation," *J. Adv. Robot.*, vol. 8, no. 3, pp. 245–261, 1994.

[16] M. M. Svinin and M. Uchiyama, "Optimal geometric structures of force/torque sensors," *Int. J. Robot. Res.*, vol. 14, no. 6, pp. 560–573, 1995.

[17] H. Maekawa, K. Tanie, K. Komoriya, M. Kaneko, C. Horiguchi, and T. Sugawara, "Development of a finger-shaped tactile sensor and its evaluation by active touch," in *Proc. IEEE Int. Conf. Robotics and Automation*, June 1992, pp. 2221–2233.

[18] E. J. Nicolson and R. S. Fearing, "Sensing capabilities of linear elastic cylindrical fingers," in *Proc. RSJ/IEEE Int. Conf. Intelligent Robots and Systems*, vol. 1, 1993, pp. 178–185.

[19] T. Speeter, "A tactile sensing system for robotic manipulation," *Int. J. Robot. Res.*, vol. 9, no. 6, pp. 25–36, 1990.

[20] K. B. Shimoga and A. A. Goldenberg, "Soft robotic fingertips—Part II: Modeling and impedance regulation," *Int. J. Robot. Res.*, vol. 15, no. 4, pp. 335–350, 1996.

[21] J. S. Son and R. D. Howe, "Tactile sensing and stiffness control with multifingered hands," in *Proc. IEEE Int. Conf. Robotics and Automation*, Minneapolis, MN, Apr. 22–28, 1996, pp. 3228–3233.

[22] Y. Yamada, K. Santa, N. Tushida, and K. Imai, "Active sensing of static friction coefficient μ for controlling grasping forces," in *Proc. Int. Conf. Advanced Robotics*, Tokyo, Japan, 1999, pp. 239–242.

[23] R. D. Howe, I. Kao, and M. R. Cutkosky, "The sliding of the robot fingers under combined torsion and shear loading," *Proc. IEEE Int. Conf. Robotics and Automation*, pp. 103–105, 1988.

[24] C. Bonivento and C. Melchiorri, "Toward dextrous manipulation with the U.B. Hand II," in *Proc. 12th. IFAC World Congr.*, vol. 10, Sydney, Australia, July 19–23, 1993, pp. 185–188.

[25] E. G. M. Holweg, "Object recognition using a tactile matrix sensor," in *Proc. European Robotics and Intelligent Systems Conf., EURISCON'94*, Malaga, Spain, August 22–26, 1994.

[26] M. Erdmann, "On a representation of friction in configuration space," *Int. J. Robot. Res.*, vol. 13, no. 3, pp. 240–271, June 1994.

[27] J. W. Jameson, "Analythic techniques for automated grasp," Ph.D. dissertation, Stanford Univ., Stanford, CA, 1985.

[28] S. Goyal, "Planar sliding of a rigid body with dry friction: Limit surfaces and dynamics of motion," Ph.D. dissertation, Faculty of Grad. School, Cornell University, Ithaca, NY, 1989.

[29] L. Sciavicco and B. Siciliano, "A solution algorithm to the inverse kinematic problem for redundant manipulators," *IEEE J. Robot. Automat.*, vol. 4, pp. 403–410, Aug. 1988.

Claudio Melchiorri (M'92) was born in 1959. He received the Laurea degree in electrical engineering and the Ph.D. degree from the University of Bologna, Bologna, Italy, in 1985 and 1990, respectively.

He was appointed as an Adjunct Associate in Engineering in the Department of Electrical Engineering, University of Florida, Gainesville, in 1988 and as a Visiting Scientist in the Artificial Intelligence Laboratory, Massachusetts Institute of Technology, Cambridge, during 1990–1991. Since 1985, he has been with the Department of Electrical Engineering, Computer Science and Systems, University of Bologna, conducting research in the field of robotics and automatic control. He currently holds the position of Associate Professor in Robotics. He is the author or coauthor of approximately 100 scientific papers presented at conferences or published in journals and of three books on digital control. He is the coeditor of three books on robotics. His research interests include dexterous robotic manipulation, haptic interfaces, telemanipulation systems, advanced sensors, and nonlinear control.